

N,N'-Diamidoketenimines via Coupling of Isocyanides to an N-Heterocyclic Carbene

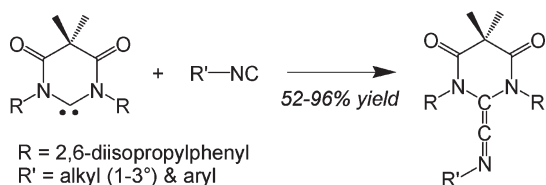
Todd W. Hudnall,[†] Eric J. Moorhead,[†] Dmitry G. Gusev,[‡] and Christopher W. Bielawski^{*†}

[†]Department of Chemistry and Biochemistry, The University of Texas at Austin, Austin, Texas 78712, and

[‡]Department of Chemistry, Wilfrid Laurier University, Waterloo, ON N2L 3C5, Canada

bielawski@cm.utexas.edu

Received March 6, 2010



Treatment of an N-heterocyclic carbene that features two amide groups N-bound to the carbene nucleus with various organic isocyanides afforded a new class of ketenimines in yields of up to 96% (isolated). DFT analyses revealed that the carbene exhibits a unique, low-lying LUMO, which may explain the atypical reactivity observed.

Ketenimines are a fascinating class of organic compounds that possess an alkene cumulated with an imine (i.e., $R_2C=C=N-R'$). Because of their unique structure and high chemical potential, they are of interest in fields that range from synthetic organic to organometallic chemistry to astrochemistry.¹ Despite this broad appeal, they remain relatively unexplored and underutilized, particularly compared to their isoelectronic ketenes, on account of synthetic limitations.² Ketenimines (see Figure 1 for representative examples) are often prepared by coupling isocyanides to suitable carbenes,

(1) (a) Schmittel, M.; Steffen, J.-P.; Ángel, M. Á. W.; Engels, B.; Lennartz, C.; Hanrath, M. *Angew. Chem., Int. Ed.* **1998**, *37*, 1562–1564. (b) Lovas, F. J.; Hollis, J. M.; Remijan, A. J.; Jewell, R. P. *Astrophys. J.* **2006**, *645*, L137–L140. (c) Sole, S.; Gornitzka, H.; Schoeller, W. W.; Bourissou, D.; Bertrand, G. *Science* **2001**, *292*, 1901–1903.

(2) (a) For a review of ketenimine chemistry, see: Krow, G. R. *Angew. Chem., Int. Ed.* **1971**, *10*, 435–449. (b) For an account of ketene chemistry, see: Tidwell, T. T. *Acc. Chem. Res.* **1990**, *23*, 273–279.

(3) (a) Igau, A.; Bacciredo, A.; Trinquier, B. G. *Angew. Chem., Int. Ed.* **1989**, *28*, 621–622. (b) Boyer, J.; Beverung, W. *J. Chem. Soc. D* **1969**, *23*, 1377–1378. (c) Merceron, N.; Miqueu, K.; Bacciredo, A.; Bertrand, G. *J. Am. Chem. Soc.* **2002**, *124*, 6806–6807. (d) Green, J.; Singer, L. *Tetrahedron Lett.* **1969**, *10*, 5093–5095. (e) Cheng, L.-Q.; Cheng, Y. *Tetrahedron* **2007**, *63*, 9359–9364. (f) Canac, Y.; Conejero, S.; Donnadiu, B.; Schoeller, W. W.; Bertrand, G. *J. Am. Chem. Soc.* **2005**, *127*, 7312–7313. (g) Busetto, L.; Marchetti, F.; Zacchini, S.; Zanotti, B. *Organometallics* **2008**, *27*, 5058–5066. (h) Despagne-Ayoub, E.; Gornitzka, H.; Bourissou, D.; Bertrand, G. *Eur. J. Org. Chem.* **2003**, 2039–2042. (i) Ciganek, E. *J. Org. Chem.* **1970**, *35*, 862–864. (j) Coy, D. H.; Haszeldine, R. N.; Newlands, M. J.; Tipping, A. E. *Chem. Commun.* **1970**, 456–457.

typically generated from their diazo or protonated precursors, or via ring-cleavage of an appropriate oxazetidine.³ Surprisingly, there are no reported examples of ketenimines derived from N-heterocyclic carbenes (NHCs), an important class of structurally and functionally diverse substrates that have been employed in a wide range of applications.⁴ This deficiency may be due to the low electrophilicities inherent to NHCs, which effectively prevents them from coupling with nucleophilic isocyanides.

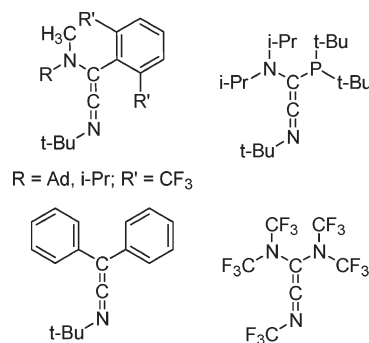


FIGURE 1. Representative examples of known ketenimines.

Recently, we reported that *N,N'*-diamidocarbene⁵ **1** displays an extraordinary degree of electrophilic characteristics. For example, **1** was found to facilitate a noncatalyzed C–H insertion reaction at a tertiary hydrocarbon and, remarkably, was capable of affixing carbon monoxide (CO) to afford a *N,N'*-diamidoketene in a reversible manner.^{5a,6} On the basis of this unusual reactivity, we reasoned that **1** should be capable of reacting with other inherently nucleophilic substrates, particularly those that are isoelectronic with CO. Herein, we demonstrate that NHC **1** couples to organic isocyanides to form *N,N'*-diamidoketenimines, a previously unknown class of molecules. In addition, we provide computational data indicating that the unusual reactivity exhibited by **1** is due to a relatively low-lying LUMO centered on the carbene atom of this molecule.

As summarized in Scheme 1, treating toluene solutions of **1** (generated in situ from its pyrimidinium precursor, [1H][OTf]; OTf = triflate) with primary, secondary, tertiary, or aryl isocyanides (1.0 equiv) afforded the desired *N,N'*-diamidoketenimines **2** in moderate to excellent yields (52–96%). Unlike the reaction of **1** with CO, the analogous reactions with

(4) (a) Bourissou, D.; Guerret, O.; Gabbaï, F. P.; Bertrand, G. *Chem. Rev.* **2000**, *100*, 39–91. (b) Ofele, K.; Tosh, E.; Taubmann, C.; Herrmann, W. A. *Chem. Rev.* **2009**, *109*, 3408–3444. (c) Diez-González, S.; Marion, N.; Nolan, S. P. *Chem. Rev.* **2009**, *109*, 3612–3676. (d) Arduengo, A. J. III *Acc. Chem. Res.* **1999**, *32*, 913–921. (e) Nair, V.; Bindu, S.; Sreekumar, V. *Angew. Chem., Int. Ed.* **2004**, *43*, 5130–5135.

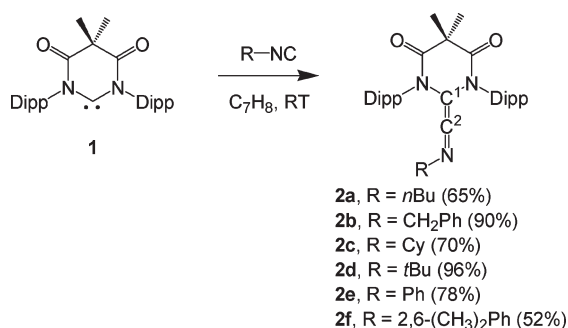
(5) (a) Hudnall, T. W.; Bielawski, C. W. *J. Am. Chem. Soc.* **2009**, *131*, 16039–16041. (b) A related *N,N'*-diamidocarbene was recently reported, see: César, V.; Lugan, N.; Lavigne, G. *Eur. J. Inorg. Chem.* **2010**, 361–365.

(6) Similar reactivities have been exhibited by cyclic alkyl amino carbenes although coupling reactions with isocyanides have not been reported, see: (a) Frey, G. D.; Lavallo, V.; Donnadiu, B.; Schoeller, W. W.; Bertrand, G. *Science* **2007**, *316*, 439–441. (b) Zeng, X.; Frey, G. D.; Kinjo, R.; Donnadiu, B.; Bertrand, G. *J. Am. Chem. Soc.* **2009**, *131*, 8690–8696. (c) Lavallo, V.; Canac, Y.; Donnadiu, B.; Schoeller, W. W.; Bertrand, G. *Angew. Chem., Int. Ed.* **2006**, *45*, 3488–3491.

TABLE 1. Selected Spectroscopic and Crystallographic Data for **2**

	${}^{13}\text{C}^1\text{N}^a$ (ppm)	${}^{13}\text{C}^2\text{N}^a$ (ppm)	ν_{CCN}^b (cm^{-1})	$d_{(\text{C}1-\text{C}2)}^c$ (Å)	$d_{(\text{C}2-\text{N}2)}^c$ (Å)	$\angle_{\text{C}1-\text{C}2-\text{N}2}^d$ (deg)
2a	198.1	108.9	2019	1.307(5)	1.240(6)	167.0(6)
2b	201.4	109.8	2014	1.318(2)	1.235(2)	176.7(2)
2c	195.4	108.0	2026	1.297(4)	1.248(4)	173.9(4)
2d	203.6	109.7	2010	1.319(2)	1.224(2)	174.8(2)
2e	205.7	111.5	2030	1.316(3)	1.230(3)	173.9(2)
2f	191.0	108.5	2024	1.328(4)	1.231(4)	173.6(3)

^aThe ${}^{13}\text{C}$ NMR chemical shifts (δ) of the emphasized atoms noted were acquired in C_6D_6 . ^bIR spectra were obtained as KBr pellets. The frequency noted was attributed to the $\text{C}^1=\text{C}^2=\text{N}$ group in the respective product. ^cDistance between the noted atoms in the respective product. ^dAngle between the noted atoms in the respective product.

SCHEME 1. Syntheses of Ketenimines **2**^a

^aCy = cyclohexyl. Dipp = 2,6-(*i*Pr)₂Ph. Isolated yields are indicated in parentheses.

the aforementioned isocyanides did not appear to be reversible. On the contrary, the products formed from these coupling reactions were thermally robust and exhibited melting points of 193–242 °C. The products were also found to be stable to air and moisture, which facilitated their isolation as pale- to dark-yellow solids.

The IR spectra of **2** revealed sharp bands at 2010–2030 cm^{-1} (KBr) which were consistent with a $\text{C}=\text{C}=\text{N}$ stretching mode typical of ketenimine functional groups (1962–2040 cm^{-1}); see Table 1.^{1–3} Likewise, the ${}^{13}\text{C}$ NMR spectra of **2** exhibited resonances at δ 190–204 and 108–110 ppm (C_6D_6) which were attributed to the nitrile CCN and carbenoid CCN carbon nuclei, respectively. Although the former chemical shifts were consistent with previously reported ketenimines (δ 160–200 ppm),³ the latter were relatively downfield (the ${}^{13}\text{C}$ CCN resonances of known ketenimines typically fall in the range of 45–65 ppm).³ The discrepancies are presumably due to the two electronegative heteroatoms bound to the carbon nucleus under interrogation. Bertrand's phosphino-amino ketenimine, which was reported to display a ${}^{13}\text{C}$ resonance at δ 94.0 ppm, provided additional support for this assignment.^{3c}

X-ray diffraction analyses performed on single crystals of **2** confirmed the structures of the desired ketenimine products (a representative example is shown in Figure 2; see the SI for additional structures) and key data are summarized in Table 1. In all cases, short C1–C2 and C2–N2 distances were observed (1.297(4)–1.328(4) and 1.224(2)–1.248(4) Å, respectively), consistent with substantial multiple bond character for each of these linkages. Moreover, the C1–C2–N2 angles were nearly linear (167.0(6)–176.7(2)°) and in good

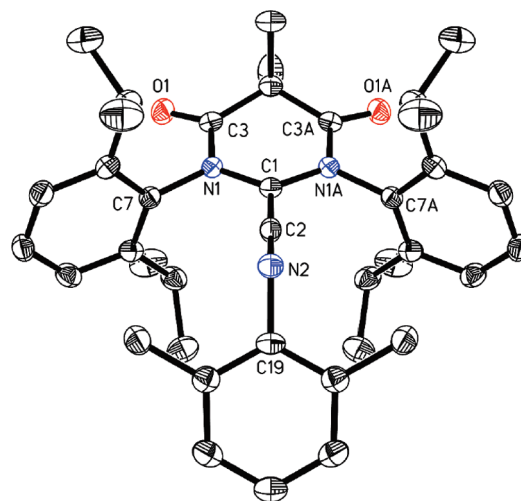


FIGURE 2. ORTEP view of the crystal structure of **2f** (50% thermal ellipsoids; hydrogen atoms have been omitted for clarity). Selected bond lengths (Å) and angles (deg): C1–C2 1.328(4), C2–N2 1.231(4), N2–C19 1.450(3), N1–C1 1.402(2), N1–C3 1.376(2), C3–O1 1.210(2), C1–C2–N2 173.6(3), C2–N2–C19 122.1(2), N1–C1–N1A 116.1(2), N1–C3–O1 120.76(17).

agreement with analogous angles exhibited by other ketenimines in the solid state.^{3g,7,8}

To gain insight into the unusual reactivity exhibited by **1**, a series of DFT calculations were performed at the PBE0/6-311+G(d,p) level of theory⁹ on a range of NHCs and their CN^tBu coupled products.¹⁰ Emphasis was placed on comparing **1**, as well as a truncated version that features *N*-methyl substituents (**3**), with two prototypical NHCs: 1,3-dimethylimidazolinyldene (**4**) and 1,3-dimethylimidazolylidene (**5**).¹¹ As summarized in Table 2, the change in enthalpy of the coupling reactions involving **1** and **3** with CN^tBu was found to be significantly more favored than analogous reactions involving **4** and **5**.¹² Supporting this assessment, the DFT

(9) Adamo, C.; Barone, V. *J. Chem. Phys.* **1999**, *110*, 6158–6170.

(10) For additional computational analyses and detailed discussions of the electronic structures of NHCs, see: (a) Heinemann, C.; Thiel, W. *Chem. Phys. Lett.* **1994**, *217*, 11–16. (b) Arduengo, A. J. III; Dias, H. V. R.; Dixon, D. A.; Harlow, R. L.; Klooster, W. T.; Koetzle, T. F. *J. Am. Chem. Soc.* **1994**, *116*, 6812–6822. (c) Arduengo, A. J. III; Bock, H.; Chen, H.; Denk, M.; Dixon, D. A.; Green, J. C.; Herrmann, W. A.; Jones, N. L.; Wagner, M.; West, R. *J. Am. Chem. Soc.* **1994**, *116*, 6641–6649. (d) Boehme, C.; Frenking, G. *J. Am. Chem. Soc.* **1996**, *118*, 2039–2046. (e) Heinemann, C.; Müller, T.; Apeloig, Y.; Schwarz, H. *J. Am. Chem. Soc.* **1996**, *118*, 2023–2038. (f) Tukov, A. A.; Normand, A. T.; Nechaev, M. S. *Dalton Trans.* **2009**, 7015–7028.

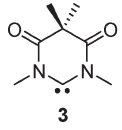
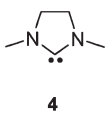
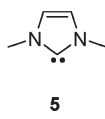
(11) See SI for additional information and further discussion.

(12) In agreement with the computational analyses, 1,3-dimesitylimidazol-2-ylidene exhibited no reactivity toward an assortment of isocyanides under various conditions (solvents, temperatures, etc.) whereas analogous reactions involving 1,3-dimesitylimidazol-2-ylidene formed complex mixtures of unidentifiable products.

(7) Jochims, J. C.; Lambrecht, J.; Burkert, U.; Zsolnai, L.; Huttner, G. *Tetrahedron* **1984**, *40*, 893–903.

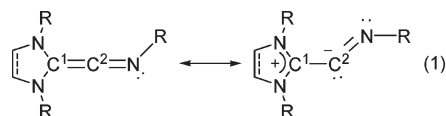
(8) Ruiz, J.; Riera, V.; Vivanco, M.; Lanfranchi, M.; Tiripicchio, A. *Organometallics* **1998**, *17*, 3835–3837.

TABLE 2. Selected Calculated Data^a

					
	$-\Delta H^b$ (kcal/mol)	$d_{(C1-C2)^c}$ (Å)	$d_{(C2-N2)^c}$ (Å)	$\angle_{C1-C2-N2}^d$ (deg)	ΔH_{S-T}^e (kcal/mol)
1	38.0	1.324	1.218	176.1	41.8
3	34.0	1.328	1.222	166.5	45.2
4	16.2	1.325	1.239	156.4	68.6
5	7.40	1.396	1.262	132.0	81.1

^aThe DFT calculations were performed at the PBE0/6-311+G(d,p) level of theory. ^bChange in enthalpy associated with the reaction: NHC + CN^tBu → NHC=CN^tBu, thermal corrections obtained from frequency calculations performed on optimized geometries were applied. ^cDistance between the noted atoms in the product NHC=CN^tBu. ^dAngle between the noted atoms in the product NHC=CN^tBu. ^eChange in enthalpy between the singlet and triplet states of the respective NHC.

optimized structure of **2d** was in excellent agreement with that determined experimentally. The optimized geometries of the calculated ketenimines formed from **4** and **5** feature relatively acute C¹–C²–N bond angles and were accompanied with significant charge buildup on the C² atom (see the SI). As such, they can be expected to adopt charge separated states (see eq 1) which may contribute to their relatively high energies. These effects may be exacerbated in the *N,N'*-diamidoketenimine derived from **5** and CN^tBu, due to a preference of the NHC-derived moiety to retain aromaticity.¹⁰



Considering compounds **3–5** were calculated to exhibit relatively large singlet–triplet gaps (ΔH_{S-T}), minimizing the possibility of radical-based coupling mechanisms with isocyanides, subsequent efforts turned toward examining the molecular orbitals of these systems to gain additional insight into the unique reactivity of **1**. Figure 3 depicts the frontier molecular orbitals of carbenes **3–5**. The relevant HOMOs of these systems were calculated to be of similar energies, suggesting that they each can be expected to display similar nucleophilicities. Indeed, various *N,N'*-diamidocarbene were previously reported to couple to electrophilic substrates, including transition metals and CS₂, in a manner similar to typical NHCs.⁵ However, the LUMO of **3**, which features an empty p-orbital on the carbene nucleus, was calculated to lie at a significantly lower energy than the corresponding LUMOs of **4** and **5**. We believe this unique MO enhances the electrophilicity exhibited by **1** and explains its reactivity toward isocyanides, carbon monoxide, and potentially other nucleophiles.¹³

In conclusion, we report the first coupling reaction between an NHC and an isocyanide. The reaction, which was enabled by **1**, was found to proceed smoothly with a range of isocyanides and facilitated access to a novel class of keteni-

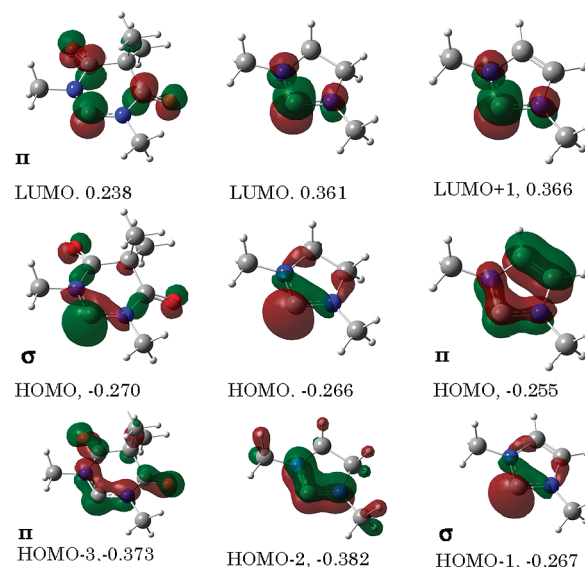


FIGURE 3. Selected molecular orbitals (MOs) of **3** (left), **4** (middle), and **5** (right) optimized at the HF/STO-3G level of theory. The values listed are the energies of the respective MO in hartrees.

mines. DFT analyses revealed that a unique low-energy LUMO inherent to **1** enhances its electrophilicity and provides an explanation for the unusual reactivity observed. On a broader level, the coupling chemistry described herein effectively expands the limited number of nonmetal catalyzed C=C bond forming reactions^{4c} and is expected to facilitate access to a spectrum of structurally and functionally diverse organic molecules of broad interest. Efforts directed toward exploring the chemistry of the ketenimines described above are underway and will be reported in due course.

Experimental Section

General Procedure for the Synthesis of **2.** To a freshly prepared solution of **1** in 5 mL of toluene (generated in situ via deprotonation of [1H][OTf]^{5a} with 1.0 mol equiv of NaHMDS) was added 1.0 mol equiv of the corresponding isocyanide. An instantaneous color change from pale-yellow to a deep yellow-orange was observed. After the resulting solution was stirred at ambient temperature in a drybox for 12 h, the solvent was removed under reduced pressure to afford a yellow-orange powder. The crude material was purified by recrystallization

(13) It is tempting to compare the coupling reaction reported herein with NHC dimerization; see: (a) Wanzlick, H. W.; Schikora, E. *Angew. Chem.* **1960**, *72*, 494. (b) Alder, R. W.; Blake, M. E.; Chaker, L.; Harvey, J. N.; Paolini, F.; Schütz, J. *Angew. Chem., Int. Ed.* **2004**, *43*, 5896–5911. (c) Kamplain, J. W.; Bielawski, C. W. *Chem. Commun.* **2006**, 1727–1729. (d) Poater, A.; Ragone, F.; Giudice, S.; Costabile, C.; Dorta, R.; Nolan, S. P.; Cavallo, L. *Organometallics* **2008**, *27*, 2679–2681. (e) Graham, D. C.; Cavell, K. J.; Yates, B. F. *J. Phys. Org. Chem.* **2005**, *18*, 298–309. (f) Luan, X.; Mariz, R.; Gatti, M.; Costabile, C.; Poater, A.; Cavallo, L.; Linden, A.; Dorta, R. *J. Am. Chem. Soc.* **2008**, *130*, 6848–6858.

from a hydrocarbon solvent to afford analytically pure **2** as a yellow solid. The above conditions were successfully performed on multiple scales, ranging from 20 to 250 mg of [1H][OTf].

2a: mp 193–194 °C, recrystallized from hexanes; ¹H NMR (C₆D₆, 300.47 MHz) δ 0.49–0.63 (m, 7H), 1.30 (d, ³J = 6.6 Hz, 24H), 1.87 (s, 6H), 2.59 (m, 2H), 3.28 (sept, ³J = 6.9 Hz), 7.00–7.03 (m, 4H), 7.11–7.13 (m, 2H); ¹³C (C₆D₆, 150.83 MHz) δ 13.7, 19.9, 23.9, 24.7, 29.3, 30.2, 31.6, 47.3, 57.6, 108.9, 124.2, 129.9, 133.0, 168.6, 198.1; IR (KBr) ν 2018 (C=C=N), 1675 cm⁻¹ (C=O); UV-vis (CH₂Cl₂) λ_{max} = 272 nm, ε = 1.50 × 10⁴ M⁻¹ cm⁻¹; HRMS [M + H]⁺ calcd for C₃₅H₅₀N₃O₂ 544.3903, found 544.3896. Anal. Calcd for C₃₅H₄₉N₃O₂: C, 77.31; H, 9.08; N, 7.73. Found: C, 76.98; H, 8.82; N, 7.83.

2b: mp 204–206 °C, recrystallized from hexanes; ¹H NMR (C₆D₆, 300.47 MHz) δ 1.30 (d, ³J = 6.6 Hz, 24H), 1.87 (s, 6H), 3.29 (br s, 4H), 3.84 (br s, 2H), 6.14 (d, ³J = 7.8 Hz, 2H), 6.86–6.94 (m, 4H), 6.98–7.08 (m, 5H); ¹³C (C₆D₆, 75.47 MHz) δ 24.6, 29.3, 47.3, 61.8, 109.8, 127.3, 127.5, 127.9, 128.1, 128.3, 128.3, 130.1, 132.8, 136.3, 168.6, 201.4; IR (KBr) ν 2014 (C=C=N), 1671 cm⁻¹ (C=O); UV-vis (CH₂Cl₂) λ_{max} = 272 nm, ε = 1.53 × 10⁴ M⁻¹ cm⁻¹; HRMS [M + H]⁺ calcd for C₃₈H₄₈N₃O₂ 578.3747, found 578.3752. Anal. Calcd for C₃₈H₄₇N₃O₂: C, 78.99; H, 8.20; N, 7.27. Found: C, 79.04; H, 8.19; N, 7.09.

2c: mp 209–210 °C, recrystallized from *n*-pentane; ¹H NMR (C₆D₆, 300.47 MHz) δ 0.50–0.77 (m, 10H), 1.32 (d, ³J = 6.9 Hz, 24H), 1.88 (s, 6H), 2.55 (m, 1H), 3.31 (sept, ³J = 6.9 Hz, 4H), 7.01–7.04 (m, 4H), 7.11–7.14 (m, 2H); ¹³C (C₆D₆, 150.82 MHz) δ 23.4, 23.9, 24.8, 25.4, 29.4, 32.4, 47.5, 67.1, 108.0, 124.2, 127.9, 128.1, 128.3, 129.9, 133.5, 168.8, 195.4; IR (KBr) ν 2026 (C=C=N), 1675 cm⁻¹ (C=O); UV-vis (CH₂Cl₂) λ_{max} = 272 nm, ε = 1.90 × 10⁴ M⁻¹ cm⁻¹; HRMS [M + H]⁺ calcd for C₃₇H₅₂N₃O₂ 570.4060, found 570.4057. Anal. Calcd for C₃₇H₅₁N₃O₂: C, 77.99; H, 9.02; N, 7.37. Found: C, 77.73; H, 8.71; N, 7.03.

2d: mp 207–208 °C, recrystallized from hexanes; ¹H NMR (C₆D₆, 300.47 MHz) δ 0.34 (s, 9H), 1.27 (br s, 24H), 1.86 (s, 6H), 3.32 (br s, 4H), 7.00–7.03 (m, 4H), 7.10–7.13 (m, 2H); ¹³C (C₆D₆, 150.81 MHz) δ 25.2, 28.5, 29.5, 31.9, 48.1, 60.6, 108.5, 124.1, 127.9, 128.1, 128.3, 129.8, 134.3, 169.2, 191.0; IR (KBr) ν 2024 (C=C=N), 1669 cm⁻¹ (C=O); UV-vis (CH₂Cl₂) λ_{max} = 272 nm, ε = 1.47 × 10⁴ M⁻¹ cm⁻¹; HRMS [M + H]⁺ calcd for C₃₅H₅₀N₃O₂ 544.3903, found 544.3900. Anal. Calcd for C₃₅H₄₉N₃O₂: C, 77.31; H, 9.08; N, 7.73. Found: C, 77.37; H, 8.87; N, 7.55.

2e: mp 202–203 °C, recrystallized from *n*-pentane; ¹H NMR (C₆D₆, 400.27 MHz) δ 1.22 (d, ³J = 6.4 Hz, 12H), 1.29 (d, ³J = 6.8 Hz, 12H), 1.89 (s, 6H), 3.30 (sept, ³J = 6.8 Hz, 4H), 6.05 (d, ³J = 7.6 Hz, 2H), 6.66 (m, 1H), 6.73 (t, ³J = 7.6 Hz, 2H), 7.01 (d, ³J = 7.6 Hz, 4H), 7.10 (t, ³J = 7.6 Hz, 4H); ¹³C (C₆D₆, 150.82 MHz) δ 23.1, 24.7, 24.8, 29.4, 47.6, 111.5, 120.7, 124.4, 126.8, 128.3, 128.7, 130.2, 145.1, 146.9, 168.8, 205.7; IR (KBr) ν 2030

(C=C=N), 1678 cm⁻¹ (C=O); UV-vis (CH₂Cl₂) λ_{max} = 272 nm, ε = 1.48 × 10⁴ M⁻¹ cm⁻¹; HRMS [M + H]⁺ calcd for C₃₇H₄₆N₃O₂ 564.3590, found 564.3581. Anal. Calcd for C₃₇H₄₅N₃O₂: C, 78.83; H, 8.05; N, 7.45. Found: C, 78.94; H, 8.06; N, 7.41.

2f: mp 241–242 °C; recrystallized from toluene; ¹H NMR (C₆D₆, 300.47 MHz) δ 1.18 (d, ³J = 6.9 Hz, 12H), 1.19 (s, 6H), 1.27 (d, ³J = 6.6 Hz, 12H), 1.84 (s, 6H), 3.31 (sept, ³J = 6.9 Hz, 4H), 6.54–6.64 (m, 3H), 6.96–7.02 (m, 4H), 7.06–7.12 (m, 2H); ¹³C (C₆D₆, 150.84 MHz) δ 17.5, 23.2, 24.6, 29.3, 47.2, 109.7, 124.7, 125.9, 127.9, 128.1, 128.3, 129.0, 130.3, 133.1, 141.4, 147.3, 168.8, 203.6; IR (KBr) ν 2010 (C=C=N), 1684 cm⁻¹ (C=O); UV-vis (CH₂Cl₂) λ_{max} = 283 nm, ε = 2.06 × 10⁴ M⁻¹ cm⁻¹; HRMS [M + H]⁺ calcd for C₃₉H₅₀N₃O₂ 592.3903, found 592.3895. Anal. Calcd for C₃₉H₄₉N₃O₂: C, 79.15; H, 8.35; N, 7.10. Found: C, 79.31; H, 8.25; N, 7.02.

Computational Details. The calculations were carried out with Gaussian 09 (Revision A.02).¹⁴ All geometries were optimized at the PBE0⁹/6-31G(d) level and were verified to have all real harmonic frequencies by frequency calculations, which also provided thermal corrections to enthalpy and APT¹⁵ charges. The geometries were subsequently reoptimized at the PBE0/6-311+G(d,p) level. The enthalpies reported in Table 2 were obtained by combining the electronic energies from the PBE0/6-311+G(d,p) calculations with the thermal corrections from the PBE0/6-31G(d) frequency calculations. The molecular orbitals shown in Figure 3 were obtained by reoptimizing the carbenes at the HF/STO-3G level. Full symmetry (when present) was used in every calculation reported herein. Some of the values listed in Table S2 (SI) were taken from a recent report.¹⁶

Acknowledgment. This work was made possible by the generous financial support of the National Science Foundation (grant No. CHE-0645563), the Robert A. Welch Foundation (grant No. F-1621), and the facilities of the Shared Hierarchical Academic Research Computing Network. We thank Dr. V. M. Lynch for assistance with the crystal structure analyses.

Supporting Information Available: Additional experimental details, characterization data, and computational analyses. This material is available free of charge via the Internet at <http://pubs.acs.org>.

(14) (a) Gaussian 09, Revision A.2; Frisch, M. J. et al. For more information and additional references see Gaussian 09 User's Reference (www.gaussian.com/g_tech/g_ur/g09help.htm). The basis sets are available from the EMSL Basis Set Library (<http://bse.pnl.gov>). (b) Feller, D. *J. Comput. Chem.* **1996**, *17*, 1571–1586. (c) Schuchardt, K. L.; Didier, B. T.; Elsethagen, T.; Sun, L.; Gurumoorthi, V.; Chase, J.; Li, J.; Windus, T. L. *J. Chem. Inf. Model.* **2007**, *47*, 1045–1052.

(15) Cioslowski, J. *J. Am. Chem. Soc.* **1989**, *111*, 8333–8336.

(16) Gusev, D. G. *Organometallics* **2009**, *28*, 6458–6461.